

Amorphous tracks in insulators induced by monoatomic and cluster ions

G. Szenes

Department of General Physics, Eötvös University, Pf. 32, H-1518 Budapest, Hungary

(Received 20 February 1998; revised manuscript received 28 December 1998)

Amorphous tracks induced by monoatomic and cluster ion beams are compared in LiNbO_3 and $\text{Y}_3\text{Fe}_5\text{O}_{12}$. In agreement with the prediction of our model, at high energy deposition $R_e^2/S_e = \text{const}$ (R_e is the effective track radius, S_e is the electronic stopping power) for monoatomic and cluster ion irradiations. This indicates that the considerably higher energy density in the experiments with cluster ion beams does not modify the track formation. The analysis shows that the width of the thermal spike does not depend on the ion velocity in the range 0.02–20 MeV/nucleon. On the other hand, a strong variation of the efficiency of the energy deposition into the thermal spike g is observed around 2 and 4 MeV/nucleon for LiNbO_3 and $\text{Y}_3\text{Fe}_5\text{O}_{12}$, respectively. The results cannot be explained by the variation of the δ -electron distribution with the specific ion energy E . The importance of the electron-lattice ion and ion-ion interactions are emphasized. The relative shift of the $g(E)$ curves is related to the different fraction of heavy elements in the two insulators. [S0163-1829(99)04129-6]

I. INTRODUCTION

Swift heavy ions induce amorphous tracks in the electronic stopping regime in many insulating crystals. An amorphous track is the final result of the interaction of the bombarding particle with the solid target. Thus, the analysis of the formation of tracks can provide important information about the processes transferring the ion energy to the target atoms.

Recently a phenomenological model was elaborated which revealed a high degree of uniformity in track formation in insulators.^{1–3} The model has been applied to all systematic data on amorphous tracks and good agreement was observed with the predictions. The reliable predictions are very important because of the growing role of energetic ions in industrial technologies, medicine, and scientific research. The results reported in this paper can be useful for other fields of the interaction of energetic ions with matter, such as inelastic sputtering, biological cell inactivation, and also for studies of tracks in polymers.

In Refs. 4 and 5–7 track studies were extended to higher values of the electronic stopping power S_e by irradiating yttrium iron garnet (YIG) and lithium niobate (LN) samples with cluster ion beams. These experiments considerably broadened the range of specific ion energies E , which is an important parameter of track formation. In this paper our phenomenological thermal spike model is used to analyze the track data. Our main interest is (i) to analyze and to compare the damage cross sections measured by cluster and monoatomic ion irradiations, (ii) to check the behavior of the parameters of our model g and $a(0)$ in a broad range of the projectile velocity.

In all figures the track data will be presented according to the analytical equations of the model, and we often refer to some general features of track formation in insulators, which we previously have deduced. Therefore, it is reasonable to start with a brief review of the model and of some results which are relevant to this paper.

II. PRESENTATION OF THE EXPERIMENTAL DATA

A. The model

We assume that as a result of the energy deposition along the trajectory of the bombarding particle a considerable local temperature increase $\Delta T(r, t)$ is induced, which can be described by a radial Gaussian distribution. An important parameter of this distribution is the initial width $a(0)$, which is attained at $t=0$, when the peak temperature is the highest.^{1,2} The target material is melted in that region, where the temperature exceeds the melting point $T_m < \Delta T(r, t) + T_{\text{ir}}$ where T_{ir} is the irradiation temperature. Due to the extremely high cooling rate an amorphous phase can be formed from melt producing a track of the particle.

The model provides the following analytical relations between the effective track radius R_e and the electronic stopping power of the bombarding ion S_e :¹

$$R_e^2 = a^2(0) \ln(S_e/S_{e_t}), \quad 0 < R_e \leq a(0) \quad (1)$$

$$R_e^2 = g S_e / (2.7 \pi \rho c T_0), \quad a(0) \leq R_e \quad (2)$$

$$S_{e_t} = \pi \rho c T_0 a^2(0) / g, \quad (3)$$

where c and ρ are the average specific heat and the density, respectively, $T_0 = T_m - T_{\text{ir}}$, and $g S_e$ is the fraction of S_e covering the thermal energy (g is the efficiency). Tracks are formed above a threshold electronic stopping power S_{e_t} . In the process of cooling the melted volume may shrink for $t > 0$ [Eq. (1)] or shrinks after an initial growth [Eq. (2)]. We refer to the logarithmic regime or the initial stage of track formation when Eq. (1) is valid and use the expression linear regime for the range of validity of Eq. (2).

We have analyzed the systematic experimental data published in the literature about the formation of amorphous tracks including various magnetic oxides,² SiO_2 quartz,³ mica, LN,⁸ and high- T_c superconductors.⁹ The main results are the following: (i) the validity of Eqs. (1) and (2) was confirmed,^{2,3} (ii) the relation between S_{e_t} and the thermal properties of the target was proved,² (iii) at high ion veloci-

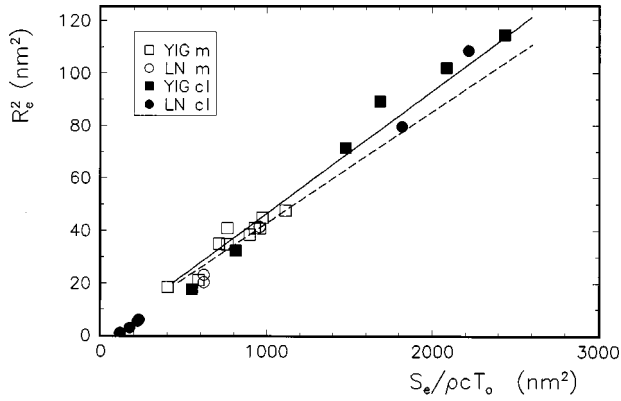


FIG. 1. Tracks induced in $\text{Y}_3\text{Fe}_5\text{O}_{12}$ (YIG) and LiNbO_3 (LN) by cluster (cl) and monoatomic (m) ion beams with $E < 2$ MeV/nucleon. The solid and the dashed lines are fits according to Eq. (2) with and without cl data (Ref. 3), respectively. Only data with $R_e > 4.5$ nm were taken into account in the fit of the solid line [see Eq. (2)].

ties ($E > 7.6$ MeV/nucleon) a uniform behavior was observed: $a(0) = 4.5$ nm and $g = 0.17$ for all insulators studied till now,^{2,8} (iv) at low ion velocities ($E < 2$ MeV/nucleon) $g = 0.36$.^{2,3} An important consequence of (i) is the method of scaling tracks measured in different materials. In this paper we also make use of this possibility.

By applying Eqs. (1)–(3) amorphous track sizes can be predicted at high ion velocities without adjustable parameters. The uniform behavior of insulating crystals in terms of the $a(0)$ and g parameters is an indication that these are the relevant parameters of the process.

B. Experimental data

Recently, two insulating crystals YIG and LN were irradiated at room temperature with various cluster beams.^{4,5–7} Previously, a large number of monoatomic ion irradiation experiments were reported on these crystals in a broad velocity range, including irradiations with low velocity ions, as well ($E < 2$ MeV/nucleon).^{10,11} This is important, since high velocity ions with the same electronic stopping power induce smaller tracks, because of the damage cross section velocity effect (briefly velocity effect).¹⁰ Therefore, they are not directly comparable to the cluster ion irradiation data.

In Ref. 3 we already analyzed low velocity track data in YIG and LN taken from Ref. 10 and Refs. 11, 12, respectively, and now they are completed in Fig. 1 with new results for YIG (Ref. 13) and also with cluster irradiation data reported in Refs. 4 and 5–7. To compare appropriately the track evolution in different insulators in the linear regime of track evolution, S_e is scaled by $\rho c T_0$ according to Eq. (2). This method of scaling is justified by the coherent behavior of YIG and LN data in this presentation.

In Refs. 3 and 14 we showed that the linearity required by Eq. (2) is clearly followed by the data, obtained by irradiation with monoatomic ion beams (dashed line in Fig. 1). When tracks induced by cluster ions are also included in the analysis, the data also follow Eq. (1) with a somewhat higher slope. We note that tracks in different materials were compared in Fig. 1, different methods [Rutherford backscattering

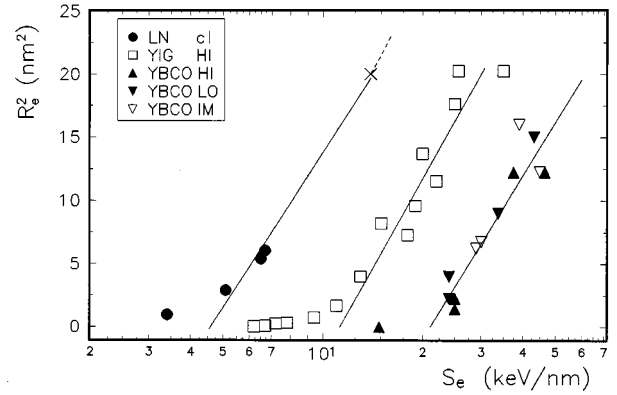


FIG. 2. Variation of the track size in $\text{Y}_3\text{Fe}_5\text{O}_{12}$ (YIG), LiNbO_3 (LN), and in a high- T_c superconductor Y-Ba-Cu-O (LO is $E < 2$ MeV/nucleon, HI is $E > 7.6$ MeV/nucleon, IM is 2 MeV/nucleon $< E < 7.6$ MeV/nucleon). The cross and the dashed line are extrapolations from Fig. 1. Irradiations were performed with cluster ions (cl) and monoatomic ions (all others), as well.

in channeling geometry (c-RBS) and high-resolution electron microscopy (HREM)] were used for track size measurements after monoatomic and cluster ion irradiation, and the TRIM code also could lead to a systematic error.

In Fig. 2 three sets of data were plotted. The tracks in YIG were induced by monoatomic projectiles with $E > 7.6$ MeV/nucleon.^{10,13} The curve describes a typical evolution of amorphous tracks for insulators. Other insulators can be characterized with the same $a(0)$ and g values in this range. For the mean value $a(0) = 4.5$ nm was obtained both from the slope and from the S_{et} values.²

A second set of data was measured in a high- T_c superconductor Y-Ba-Cu-O. It was observed by Zhu *et al.*¹⁵ that the track size is sensitive to the direction of the beam with respect to the crystallographic axes, and also to the oxygen concentration of the $\text{YBa}_2\text{Cu}_3\text{O}_{7-\delta}$ samples. To have a coherent data basis we selected those experiments, in which electron microscopy or Mössbauer spectroscopy were used to measure the track size, the ion beam was parallel to the c direction of the Y-Ba-Cu-O crystal and $\delta \leq 0.1$. After such a selection a further difficulty is that the irradiations were performed either at 300 or at 80 K. Thus, the $T_0 = T_m - T_{ir}$ values were different. To solve this problem a reference temperature $T = 80$ K was chosen. Then Eq. (1) was applied to calculate the value of S_e^* , which would be necessary to induce at $T_{ir} = 80$ K a track with the same radius, which was induced by S_e at $T_{ir} = 300$ K. By applying Eq. (1) we found $S_e^* = 1.14 S_e$ when the temperature dependence of the specific heat was also taken into account. The details of this procedure were given in Ref. 9. The experimental data are summarized in Table I, where the corrected S_e values and the references are also given.^{16–26}

It is remarkable that all track data measured in Y-Ba-Cu-O follow the same line in Fig. 2, including those with $E < 2$ MeV/nucleon and $E > 7.6$ MeV/nucleon, i.e., no velocity effect is observed. By applying Eq. (1) we obtain $a(0) = 4.32$ nm which is valid for irradiation with low and high velocity ions, as well and which has a close value to $a(0) = 4.5$ nm found in insulators.²

TABLE I. Tracks induced in $Y_3Ba_2CuO_{7-\delta}$ with $\delta \leq 0.1$; T_{ir} , R_e , and E , are the irradiation temperature, the effective track radius, and the specific ion energy, respectively. The temperature correction was made according to $S_e^* = 1.14 S_e$ for $T_{ir} = 300$ K (see text). The applied methods were transmission electron microscopy (TEM), high-resolution electron microscopy (HREM), and Mössbauer spectroscopy (Möss).

| S_e (keV/nm) | T_{ir} (K) | S_e^* (keV/nm) | R_e^2 (nm ²) | E (MeV/n) | Method | Ref. |
|-------------------|-----------------|---------------------|-------------------------------|----------------|--------|-------------------|
| 13 | 300 | 14.8 | 0 | 43 | TEM | 16 |
| 22 | 300 | 25 | 1.44 | 27 | Möss | 17 |
| 22 | 300 | 25 | 2.25 | 27 | TEM | 17 |
| 33 | 300 | 37.5 | 4.00 | 25 | TEM | 18 |
| 41 | 300 | 46.6 | 12.25 | 10–25 | HREM | 18 |
| 40 | 80 | 40 | 12.25 | 4.3 | HREM | 19 |
| 30 | 80 | 30 | 6.76 | 3.9 | Möss | 20 |
| 39 | 80 | 39 | 16.00 | 3.7 | HREM | 21 ^{a,b} |
| 29 | 80 | 29 | 6.25 | 2.6 | HREM | 21 ^{a,b} |
| 38 | 300 | 43.2 | 15.00 | ~2 | TEM | 22,23 |
| 24 | 80 | 24 | 2.25 | 1.3 | HREM | 24 |
| 24 | 80 | 24 | 4.00 | 1.3 | HREM | 25 ^b |
| 28 | 300 | 31.8 | 9.00 | 0.8 | HREM | 26 |

^a T_{ir} is estimated, it is not explicitly given in the reference.

^b δ is estimated, it is not explicitly given in the reference.

Track data in the third set were obtained by irradiation of LN by cluster ions.^{5–7} Recently, Ramos *et al.* performed experiments on LN with Cl and Br ions of 5–10 MeV.²⁷ These data are not shown in Fig. 2 because they were deduced by assuming a multiple-hit mechanism of the induced lattice disorder which is different from that which was applied in the case of other data. We discuss this problem later.

Unfortunately, all these tracks are small. So they are not suitable for the determination of $a(0)$ from the shape of the $R_e^2 - S_e$ curve. However, it is advantageous to use them for the estimate of S_{et} . Therefore, we completed them with an estimated track size, (denoted by a cross in Fig. 2), which was extrapolated from cluster data by using the plot in Fig. 1. We also show in Fig. 2 that part of the line in Fig. 1 which should be joined. This helps us to determine the value of S_{et} more accurately. By this method we got $S_{et} = 4.60$ keV/nm. When the other parameters in Eq. (3) are known then $a(0)$ can be estimated at very low ion velocities.

Presently, the range of the specific energy E extends three orders of magnitude, where amorphous tracks were studied in insulators. In Fig. 3 the variation of the efficiency g is plotted versus E . The g values were determined by using Eqs. (1) and (3) and Eq. (2) for tracks with $1.65 \text{ nm} < R_e < 4.5 \text{ nm}$ and $R_e > 4.5 \text{ nm}$, respectively. The data were taken from Refs. 4, 10, 13, and 28 (YIG) and Refs. 5–7, 11, and 12 (LN). When different parameters are given in Refs. 10, 13, and 28 for the same experiments (e.g., ⁶³Cu, $E = 0.8$ MeV/nucleon or ⁸⁴Kr, $E = 2.8$ MeV/nucleon) the track data in the original publications were taken into consideration.

In Fig. 3 the solid lines are not the result of a fit, they are to guide the eye. The individual experimental points show a considerable scatter. In such difficult experiments we do not attribute high significance to large deviations which some-

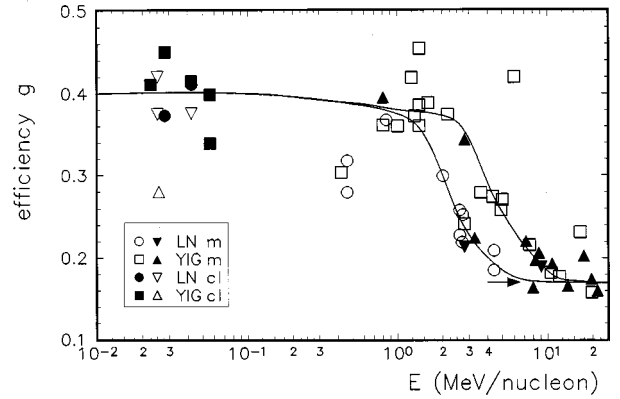


FIG. 3. Variation of the efficiency g with the specific ion energy E in $Y_3Fe_5O_{12}$ (YIG) and $LiNbO_3$ (LN). The solid lines are to guide the eye. The g values were calculated by applying Eqs. (1), (3) (triangles) and Eq. (2) (all others) to tracks induced by monoatomic (m) and cluster ion (cl) beams. The arrow shows the average efficiency for insulators at high ion velocities (Ref. 2).

times occur. Usually, the density of track data is always sufficient to show clearly the shape of the curve. It is remarkable how smoothly the efficiency values are joined, in spite of the fact that they were determined by different methods [Eqs. (1) and (3) and Eq. (2)] from different data sets. We note that we used track data in the range $2.9 \text{ nm}^2 < R_e^2 < 115 \text{ nm}^2$ of different materials and the variation of the efficiency g shows a coherent picture.

The arrow in Fig. 3 shows the common value of the efficiency $g = 0.17$ at high ion velocities. This value was deduced from all published systematic track data with $R_e < a(0)$ measured in various insulators. Since a large number of tracks were analyzed, the statistical error is small. It follows from our previous results that the solid lines in Fig. 3 should join this level.¹⁴

III. DISCUSSION

A. Track evolution in monoatomic and cluster ion irradiation experiments

In experiments with cluster ion beams, tracks are formed in conditions when the deposited energy can be very high and the velocity of the projectile is low. As a result, the energy density of the δ electrons can be much higher than that which occurs when the irradiation is performed with monoatomic ion beams. If the energy density is of importance for the process of track formation, then significant quantitative differences between the two experiments are expected.

Previously, we found a linear regime of track evolution for tracks induced by low velocity monoatomic ion beams.^{3,14} In this case, the efficiency can be simply found, because the slope of the line depends on g and the materials parameters, and does not depend on $a(0)$ [see Eq. (2)]. All tracks should be taken into account in the range of validity of Eq. (2) $R_e > a(0)$. Later we shall show in this paper that the variation of $a(0)$ with E can be neglected. Therefore, we expect for tracks induced by cluster beams that as S_e is reduced, the linear regime [Eq. (2)] is changed to a logarithmic one [Eq. (1)] also at about $R_e = 4.5 \text{ nm}$.

In Fig. 1 tracks induced by monoatomic and cluster ion beams were compared. We estimated the efficiency g from the slope of the solid line by applying Eq. (2) and $g=0.39$ was found. When obtaining this value tracks with $R_e < 4.5$ nm were not taken into account, because the linear regime of the track formation is valid only for $R_e > 4.5$ nm [see Eq. (2)]. Previously, $g=0.36$ was estimated from tracks induced by monoatomic beams (dashed line) at about $E = 1-2$ MeV/nucleon. Thus, we conclude that the efficiencies for YIG and LN agree within experimental error at $E = 0.02$ MeV/nucleon and at $E = 1$ MeV/nucleon.

We emphasize that the good correlation between the results of the monoatomic and cluster beam experiments was achieved without adjustable parameters. The scaling by $\rho c T_0$ also worked well.

The close values of the efficiencies in monoatomic and cluster ion irradiation experiments show that the high initial energy density in cluster irradiation experiments does not lead to new contributions to the energy transfer. This indicates that there is no change in the mechanism of energy transfer to the matrix, when tracks are induced by cluster ions.

There are no reliable theoretical methods for the calculation of the electronic energy losses of cluster ions and until now only few measurements were performed. Usually, the validity of the superposition is assumed and S_e of a cluster ion is calculated by simply summing the electronic stopping power appropriate for individual carbon atoms. The S_e values which we used in Fig. 1 were calculated by the same procedure. The good correlation between the damage cross sections in monoatomic and cluster ion irradiation experiments is indirect evidence that the principle of superposition or the sum rule is valid for the electronic energy losses of cluster ions. This is a by-product of our results. A systematic parallel study of the evolution of track sizes in monoatomic and cluster beam experiments could lead to even more convincing results.

Dunlop *et al.* performed a systematic investigation of the evolution of the shape of tracks as the cluster slowed down in the target.⁴ They often observed the separation of the tracks into two or three branches. This branching was related to the fractioning of the C_{60} particle. As Fig. 1 proves, our model gives a correct analytical relation between R_e and S_e . Thus, S_e can be estimated from the size of the branch. On the other hand, the electronic stopping power per carbon atom can be determined from the track length at the separation. By comparing the two values the number of carbon atoms in the fragment can be simply found. Such a procedure can be easily performed having precise data, obtained by high-resolution electron microscopy.

B. The dependence of the initial width of the temperature distribution $a(0)$ on the specific ion energy E

In a general case, our model has two free parameters $a(0)$ and g . Previously, we found for $E > 7.6$ MeV/nucleon that $g=0.17$ and $a(0)=4.5$ nm for insulators.² Thus, we are able to predict track sizes for high velocity ion irradiation experiments without adjustable parameters. If the value of $a(0)$ were known, the same could be made in the low velocity range. As Eq. (2) does not depend on $a(0)$, this parameter

can be determined from Eq. (1) or Eq. (3). Therefore, tracks with large radii are not useful for this analysis. In Fig. 2 the results of the irradiation experiments on LN with cluster and monoatomic ions were plotted^{5,7} and $S_{et}=4.60$ keV/nm was found.

We have already mentioned that recently, Ramos *et al.* performed c-RBS measurements on LN samples irradiated by 5–10 MeV Cl and Br ions. When they analyzed the variation of the relative disorder α with the fluence, the data showed a deviation from the Poisson law above about $\alpha \approx 0.25-0.3$. Therefore, the analysis was performed based on a multiple-hit mechanism, instead of the single-hit mechanism, which has been most often used for processes where the defect creation is in correlation with S_e . They deduced about three times higher damage cross sections A_e compared to those for irradiation with C_6 , C_8 cluster beams at similar values of the electronic stopping power.⁵ We note that such a comparison was not made in Ref. 27, and previously, no deviations from the Poisson law were observed in experiments with cluster ions.

We analyzed the experimental data reported in Ref. 27 in the range $\alpha < 0.25-0.3$, where the deviations from the Poisson law are small, and we estimated the damage cross section from the slope of the evolution of the relative disorder α with the fluence. The damage cross sections for irradiation with 5–10 MeV Cl, Br ions and C_6 , C_8 cluster ions agree within experimental error if this procedure is applied. The efficiency g was also evaluated and $g=0.4-0.415$ was obtained which is in good agreement with $g=0.39$ deduced from Fig. 1.

It is difficult to explain these agreements, and to understand why one would operate a different mechanism in the same range of the electronic stopping power for low velocity Cl, Br, and C_6 , C_8 cluster ion irradiations, and why there is a change in the mechanism at about $S_e=8$ keV/nm, which does not depend on the velocity of the projectiles, as predicted in Ref. 27 for monoatomic ions. Our opinion is that HREM studies and irradiation experiments up to the complete amorphization of LN samples by cluster ions in controlled experimental conditions can provide useful information for the solution of this problem.

In Fig. 2 the lines corresponding to irradiation experiments with high velocity (YIG) and low velocity (LN) ions are nearly parallel indicating that the values of the $a(0)$ parameter are quite close. This observation was definitely confirmed by the estimation of $a(0)$ for LN applying Eq. (3). The temperature variation of the specific heat was calculated using the experimental data of Zhdanova *et al.*²⁹ The Dulong-Petit value $c=850$ J/kg K was accepted for 500 K $< T < 1523$ K and $c=830$ J/kg K was obtained for the average specific heat between 300 K and T_m . When $\rho = 4650$ kg/m³, $T_m = 1523$ K, $T_{ir} = 300$ K, and $g=0.39$ are introduced into Eq. (3), $a(0)=4.40$ nm is obtained. This value agrees within experimental error with that obtained for 7.6 MeV/nucleon $< E < 20$ MeV/nucleon.² This proves that the initial width of the temperature distribution $a(0)$ is independent from the specific ion energy E for 0.02 MeV/nucleon $< E < 20$ MeV/nucleon. We emphasize that we arrived at this conclusion by a highly transparent analysis, and this result is clearly demonstrated in Fig. 2 by the parallel course of the lines. Although $a(0)$ could not be

determined for YIG with cluster irradiation, we have little doubt that the behavior of YIG and LN agree in this respect in this velocity range.

This conclusion has practical importance besides the theoretical consequences. Since $a(0)$ is constant for insulators, only a single parameter, the efficiency g , is required to describe track evolution at any S_e and E values. Moreover, the efficiency g varies only in a narrow range of E , outside this range it is also constant. Thus, the prediction of S_{et} and of the track sizes outside this range require only the knowledge of ρ , c , and T_m . On the other hand, as $a(0)=\text{const}$, the variation of the efficiency g alone provides information about the velocity effect, and this information can be easily obtained from track data with $R_e < a(0)$, as well. Thus, light projectiles with low S_e values can be used more often in the future in irradiation experiments.

Our result means that the initial width of the temperature distribution $a(0)=\text{const}$ for low and high velocity irradiations, as well. The thermal energy gS_e is proportional to the product $a(0)T_p$ where T_p is the peak temperature at $t=0$ (in subsequent moments the peak temperature gradually decreases because of the heat conduction). Thus, when the specific ion energy E decreases from a high value, only T_p varies and it increases by about a factor of two when E is reduced from 20 to 1–2 MeV/nucleon. This explains why S_{et} is reduced for low velocity irradiations and why the tracks are smaller in experiments with high velocity ions at equal values of S_e .

The analysis presented in this paper clearly showed that track sizes in LN and YIG can be correctly predicted by Eqs. (1)–(3) in a broad velocity range. Our opinion is that the general features observed in LN and YIG must be characteristic to a large number of other insulating materials. A difference is expected in the range where g steeply varies, because the position and shape of the drop in $g(E)$ may be different for various projectile-target combinations.

C. Analysis of the velocity effect

It is widely accepted that track formation cannot be described by S_e alone because of the velocity effect. Dunlop *et al.* claimed that the volumic energy density $P = S_e / (\pi R_e^2)$ is a more relevant parameter than S_e .⁴ In Ref. 30 we already showed that P varies with the track size even if one could keep the ion velocities constant in irradiation experiments with various S_e values. Now, we can demonstrate this. Actually, for irradiation of LN with C_{60} (Ref. 6) ($E=0.042$ MeV/nucleon, $S_e=65$ keV/nm, $R_e^2=108$ nm²) and C_6 (Ref. 5) beams ($E=0.042$ MeV/nucleon, $S_e=6.5$ keV/nm, $R_e^2=5.4$ nm²) $P=191$ and 382 eV/nm³, respectively. In this case P varies by a factor of 2, though there is no contribution from the velocity effect, as the E values are identical. The difference is even higher for a smaller track induced by C_6 (Ref. 7) cluster ions ($E=0.025$ MeV/nucleon, $S_e=5.1$ keV/nm, $R_e^2=2.87$ nm²) since $P=566$ eV/nm³ in this case. The corresponding g values are shown in Fig. 3 and they agree within 10% for these tracks.

The consequence of the velocity effect is the shift of the R_e^2 - S_e curve to lower S_e values¹⁰ forming a series of curves as E gradually decreases. $P = S_e / (\pi R_e^2)$ is the slope of a line with coordinates (0,0) and $(S_e, \pi R_e^2)$. This line crosses the

series of the R_e^2 - S_e curves, and in the crossing points P is equal for all curves, having different E values. Thus, the variation of P cannot be in correlation with the velocity effect, because P varies when $E=\text{const}$ and $P=\text{const}$ when E varies in a broad range.

The origin of the problem with P is that the radial energy distribution in the target is not restricted to the dimensions of the track. This is the consequence of the threshold behavior of track formation. This clearly shows that the physical meaning of P is not an energy density, which really exists anywhere in the target. Our opinion is that the volumic energy density P is not suitable for the characterization of the velocity effect.

We propose to use the efficiency g for the characterization of the velocity effect. In our model g defines the fraction of S_e converted into thermal energy. We note, that this definition is not related to the track size. Although $P = (2.7\rho c T_0)/g$ in the range of validity of Eq. (2), there are significant differences between the two parameters. It is important, that at $E=\text{const}$ the efficiency g is the same for $0 < R_e < a(0)$ and $R_e > a(0)$,¹⁴ i.e., the efficiency g does not vary with S_e (or R_e). As we showed previously, this is not true for the parameter P .

The efficiency g varies only when the fraction of the energy deposited in the thermal spike increases or decreases, e.g., g is different in experiments with low and high velocity ions.¹⁴ Moreover, the value of g does not depend on the target material at high and low ion velocities.^{2,3} This is not valid for the parameter P , either. Therefore, the efficiency g is the suitable parameter for the analysis of the velocity effect.

We show in Fig. 3 the variation of the efficiency g in a broad range of the ion velocity. When analyzing the plot we note that there are some data at about 0.4 MeV/nucleon suggesting a reduction of g . In these experiments E was reduced from about 5 MeV/nucleon by relatively thick aluminum foils. However, an underestimate of the thickness by about 3% would modify the value of S_e to such an extent that no reduction of g would be supposed. Since such an underestimate is quite possible, this point must be checked and appropriate experiments are in progress.

The reduction of the efficiency between 0.02 and 20 MeV/nucleon is about 50%. Most of this reduction takes place in a relatively narrow range. The efficiency for YIG is systematically higher than that of LN for 2 MeV/nucleon $< E < 5$ MeV/nucleon, while there is a good agreement for $E < 1$ MeV/nucleon. The shape of the $g(E)$ curve is clearly determined by the data for LN, and the deviation from the mean value is small. Although the scatter of YIG data is sometimes very high, they definitely follow a single curve in the range 2 MeV/nucleon $< E < 10$ MeV/nucleon.

There are two g values in this range with high deviations from the $g(E)$ curve (open squares at $E=2.8$, and 6 MeV/nucleon), which were estimated from tracks first reported in Ref. 31. Since these deviations are nearly equal but they have opposite signs, they do not indicate a course different from the solid line in Fig. 3.

The most interesting feature of the reduction of the efficiency is that the $g(E)$ curves for YIG and LN are shifted relatively to each other. Thus, the velocity effect depends on

the composition of the target. We assume that an important feature of the composition is the fraction of heavy elements in the target molecules. In lithium niobate one heavy atom and four light atoms compose the molecule. In $Y_3Fe_5O_{12}$ the fraction of heavy elements is considerably higher. If this consideration is correct then the curve drawn for YIG in Fig. 3 is characteristic for insulating crystals in this second group. The curve for LN is in an intermediate position and an interesting question is the velocity dependence of amorphous track formation in targets without heavy elements. Until now, no experiments on such crystals have been published and we expect in such crystals a further shift of the onset of the velocity dependence to lower E values.

Presently, we do not precisely know the shape of the curves. However, the onset of the velocity dependence can be well determined and the separation of the two curves is obvious. The range of the specific energy E where a low or high efficiency is found depends on the composition of the target. Therefore, these ranges cannot be declared with a general validity. On the other hand, it was shown that in the high velocity limit $g=0.17$ even for very different materials² and the present analysis indicates that at low ion velocities $g \approx 0.4$ can be a common value.

The separation of the $g(E)$ curves for YIG and LN, the range of E where this occurs, and the magnitude of the change are important features of the underlying mechanism. Further systematic investigations and more accurate measurements of the $g(E)$ function are required for understanding the effect of the target composition, atomic mass of the projectile, and other parameters. Until now, no more information besides the bare existence of the velocity effect could be extracted from the experiments by the application of other models. The present study demonstrates an experimental possibility in the investigation of the mechanism of the interaction of energetic particles with solids. They can give a closer insight into the basic processes and important new parameters can be revealed. We will discuss later the physical consequences of the separation of the $g(E)$ curves, together with some other results.

D. Considerations about the mechanisms of the energy transfer

We already concluded in the discussion of the results plotted in Fig. 1 that the track formation is not so sensitive to the energy density of δ electrons. As $a(0)=\text{const}$ within a broad range of ion velocities, the width of the thermal spike cannot be related to the parameters of the δ -electron distribution either, which considerably vary with E . This is a rather unexpected result as a different approach is applied in the microscopic models.^{32,33} Regarding the velocity effect, Toulemonde *et al.* claim that the variations of the δ electron and the temperature distributions with E are closely related and the energy loss of the projectile is always completely converted into the thermal energy of the spike. We found just the opposite: the initial Gaussian width $a(0)=\text{const}$ and the transferred energy is changed because of the variation of the efficiency g with E . Our method of analysis was rather straightforward and no adjustable parameters were used. Therefore, we consider the conclusion concerning the constant width of the spike a reliable result.

In various materials the transport properties can modify the value of $a(0)$. We found that $a(0)=\text{const}$ for various insulators within the experimental error. This is related to the poor transport properties of insulators. In semiconductors we expect larger $a(0)$ values and its variation from target to target. Until now a track analysis was made only in semiconducting GeS, and $a(0)=11.6$ nm was obtained which is considerably larger than its value in insulators.

The width of the thermal spike $a(0)$ as well as the relatively steep variation of the efficiency in the range 1–5 MeV/nucleon cannot be related to the range of δ electrons. Meftah *et al.* estimated at various E values the radius R_d of a cylindrical volume in YIG in which 66% of the dose of δ electrons is deposited.¹⁰ According to such calculation for LN $3.5 \text{ nm} < R_d < 5 \text{ nm}$ in the range 1.5–4 MeV/nucleon where g steeply varies. This small variation of R_d cannot be responsible for the considerable reduction of g because at $E=20$ MeV/nucleon $R_d=8.6$ nm and g varies only slightly for $E > 4$ MeV/nucleon. The considerable separation of the $g(E)$ curves in Fig. 3 cannot be explained on this basis, either. We discussed this problem in more detail in Ref. 30.

In Ref. 30 we presented a numerical analysis of the fits made by Meftah *et al.*¹³ and showed that, in fact, the variation of the adjustable parameter λ with E accounts for the prevailing part of the velocity effect. In spite of the declaration of the authors, the variation of R_d with the ion velocity has only a minor contribution.

The microscopic model of Toulemonde *et al.* is based on ‘‘drastic approximations’’.¹³ Additionally, no reliable numerical values are known in the conditions of a thermal spike for important parameters of the model: thermal diffusivity, heat of fusion, specific heat, etc. It is also a rough assumption that the total energy of the projectile is converted into thermal energy of the spike. The only means to compensate the numerical consequences of the various approximations is to adjust appropriately the value of λ . Moreover, this λ parameter is also used to account for the velocity effect.

We discuss this, as recently Meftah *et al.* reported a correlation between the bandgap energy E_g and the parameter λ (Refs. 13, 34) in $BaFe_{12}O_{19}$, $Y_3Fe_5O_{12}$, $Y_3Al_5O_{12}$, and SiO_2 . Our opinion is that because of the above considerations, one must be highly cautious to attribute a physical meaning to the differences in the values of λ in various insulating crystals. It is also difficult to reconcile that on one hand, E_g is a relevant parameter of the process of track formation, and on the other hand, track evolution and S_{et} in various insulators can be scaled by $\rho c T_0$ (Refs. 2, 3) (see also Figs. 1 and 3) and correctly predicted without taking into account E_g .

The results of our analysis indicate that the interaction of δ electrons with lattice atoms is not solely responsible for the energy transfer. To account for the velocity effect other contributions must also be taken into consideration. We plotted the track sizes versus S_e for Y-Ba-Cu-O in Fig. 2 distinguishing tracks induced by beams with $E < 2$ MeV/nucleon and $E > 7.6$ MeV/nucleon and $2 \text{ MeV/nucleon} < E < 7.6 \text{ MeV/nucleon}$. In insulators the tracks induced by low and high velocity ions follow different curves, because the damage cross sections are different at equal S_e values. In Y-Ba-Cu-O, which has a metallic conduction, these curves coincide. Consequently, there is no velocity effect in the formation of amorphous tracks.³⁵ This indicates that the ve-

locity effect may be related to the type of conduction of the target, which is an important feature of the phenomenon. We assume that the absence of the velocity effect in Y-Ba-Cu-O is the consequence of the very fast screening of lattice ions by the conduction electrons. In insulators the screening time is considerably longer leading to an enhanced contribution of ion-ion and electron-ion interactions to the energy transfer to the lattice.

This point has been discussed in more detail and it is published elsewhere.³⁶ The main results are the following. After passing of the projectile, light lattice ions, like oxygen, can gain kinetic energy of 1 eV for about 2 fs through Coulomb interaction with neighboring heavy lattice ions. This energy is then partitioned among neighboring atoms.³⁷ By this mechanism part of the total electrostatic energy can be transferred directly to the atomic movement. The energy transfer by electron scattering is also enhanced when lattice atoms in the track core become highly charged ions. These two contributions depend nonlinearly on the mean ion charge and on the ion number density N_i . When the velocity of the bombarding ion decreases, N_i increases leading to an enhanced energy transfer in the track region. This can explain the increase of the efficiency g in Fig. 3. The excitation of highly charged states requires considerably lower energy for heavy atoms in the lattice points. In YIG crystal the fraction of heavy atoms is two times higher than in LN. Therefore, a higher density of highly charged ions is formed in the track for YIG than for LN at the same specific ion energy E . This leads to a more efficient energy transfer in the case of YIG compared to that of LN in the range of about $2 \text{ MeV/nucleon} < E < 5 \text{ MeV/nucleon}$. We assume that the separation of the $g(E)$ curves and the shift of the onset of the velocity effect in YIG and LN are related to this effect.

LN is the only insulator with a low fraction of heavy elements, in which amorphization has been studied in that range of E where the velocity effect appears and strongly varies. We do not know of any ion-induced amorphization experiment on crystalline insulators without heavy elements as well as without light elements. Such data could provide information about unknown features of the energy transfer processes. Cluster ion beams can be very useful in these investigations. In this respect it is important for the selection

of suitable materials, that our analysis showed that the application of our model leads to coherent results in the case of experiments with monoatomic and cluster ion beams.

IV. CONCLUSIONS

The analysis of the R_e^2 - S_e relation provides an indirect evidence of the validity of the sum rule in the calculation of the S_e of cluster ions. Damage cross sections for cluster ion irradiations can be well predicted based on the results obtained with monoatomic beams by applying a simple phenomenological thermal spike model. This shows that the high initial energy density in cluster ion irradiation experiments does not lead to additional contributions in the process of energy transfer to the lattice.

Our analysis showed for cluster ion bombardment of LN that the initial width of the temperature distribution $a(0) = 4.40 \text{ nm}$, which agrees within experimental error with $a(0) = 4.5 \text{ nm}$, the value obtained in experiments with high velocity ions.² We concluded that $a(0) = \text{const}$ in the whole range of $0.02 \text{ MeV/nucleon} < E < 20 \text{ MeV/nucleon}$. We also found that besides the material properties ρ , c , and T_m , the track size is determined only by a single parameter $g(E)$, characterizing the fraction of the deposited energy which is converted into the thermal energy of the spike. The variation of the efficiency g is considerable for YIG and LN only at $1 \text{ MeV/nucleon} < E < 5 \text{ MeV/nucleon}$ and the $g(E)$ curves are shifted relative to each other. This shift is related to the composition of the targets.

The variation of the parameters of the δ -electron distribution with the ion velocity cannot account for these observations. The results of the analysis indicate that besides the electron-atom scattering other mechanisms also contribute to the energy transfer. Electron-ion and ion-ion interactions are assumed to be responsible for the variation of the efficiency g .

ACKNOWLEDGMENT

This work was accomplished with the partial support of the National Scientific Research Fund (OTKA, Hungary) under Contracts No. T014987 and T025805.

¹G. Szenes, Mater. Sci. Forum **97-99**, 647 (1992).

²G. Szenes, Phys. Rev. B **51**, 8026 (1995).

³G. Szenes, Nucl. Instrum. Methods Phys. Res. B **122**, 530 (1997).

⁴A. Dunlop, G. Jaskierowicz, J. Jensen, and S. Della-Negra, Nucl. Instrum. Methods Phys. Res. B **132**, 93 (1997).

⁵B. Canut, S. Ramos, N. Bonardi, J. Chaumont, H. Bernas, and E. Cottureau, Nucl. Instrum. Methods Phys. Res. B **122**, 335 (1997).

⁶S. M. M. Ramos, N. Bonardi, B. Canut, and S. Della-Negra, Phys. Rev. B **57**, 189 (1998).

⁷B. Canut and S. M. M. Ramos, Radiat. Eff. Defects Solids **145**, 1 (1998).

⁸G. Szenes, Nucl. Instrum. Methods Phys. Res. B **116**, 141 (1996).

⁹G. Szenes, Phys. Rev. B **54**, 12 458 (1996).

¹⁰A. Meftah *et al.*, Phys. Rev. B **48**, 920 (1993).

¹¹B. Canut, S. M. M. Ramos, R. Brenier, P. Thevenard, J. L. Loubet, and M. Toulemonde, Nucl. Instrum. Methods Phys. Res. B **107**, 194 (1996).

¹²S. M. M. Ramos *et al.*, Nucl. Instrum. Methods Phys. Res. B **107**, 254 (1996).

¹³A. Meftah *et al.*, Nucl. Instrum. Methods Phys. Res. B **122**, 470 (1997).

¹⁴G. Szenes, Phys. Rev. B **52**, 6154 (1995).

¹⁵Y. Zhu *et al.*, Phys. Rev. B **48**, 920 (1993).

¹⁶A. Legris, F. Rullier-Albenque, A. Barbu, H. Pascard, S. Bouffard, E. Aumier, and P. Lejay, Radiat. Eff. Defects Solids **126**, 155 (1993).

¹⁷D. Bourgault, N. Nguyen, D. Groult, S. Bouffard, J. Provost, M. Y. Hervieu, M. Toulemonde, and B. Raveau, Radiat. Eff. Defects Solids **114**, 315 (1990).

- ¹⁸V. Hardy, D. Groult, M. Y. Hervieu, J. Provost, B. Raveau, and S. Bouffard, *Nucl. Instrum. Methods Phys. Res. B* **54**, 472 (1991).
- ¹⁹M. Kraus *et al.*, *Radiat. Eff. Defects Solids* **126**, 147 (1993).
- ²⁰J. Dengler *et al.*, *Hyperfine Interact.* **70**, 921 (1992).
- ²¹B. Holzapfel, G. Kreselmeyer, M. Kraus, S. Bouffard, S. Klaumünzer, L. Schultz, and G. Saemann-Ischenko, *J. Alloys Compd.* **195**, 411 (1993).
- ²²L. Krusin-Elbaum, L. Civale, G. Blatter, A. D. Marwick, F. Holtzberg, and C. Field, *Phys. Rev. Lett.* **72**, 1914 (1994).
- ²³A. D. Marwick *et al.*, *Nucl. Instrum. Methods Phys. Res. B* **80/81**, 1143 (1993).
- ²⁴H. Watanabe, B. Kabius, K. Urban, B. Roas, S. Klaumünzer, and G. Saemann-Ischenko, *Physica C* **179**, 75 (1991).
- ²⁵B. Roas *et al.*, *Europhys. Lett.* **11**, 669 (1990).
- ²⁶L. Civale *et al.*, *Phys. Rev. B* **50**, 4102 (1994).
- ²⁷S. M. M. Ramos *et al.*, *Radiat. Eff. Defects Solids* **143**, 299 (1998).
- ²⁸J. M. Costantini, F. Brisard, M. Toulemonde, and F. Studer, *Nucl. Instrum. Methods Phys. Res. B* **122**, 514 (1997).
- ²⁹V. V. Zhdanova, V. P. Klyuev, V. V. Lemanov, I. A. Smirnov, and V. V. Tikhonov, *Fiz. Tverd. Tela (Leningrad)* **10**, 1725 (1968) [*Sov. Phys. Solid State* **10**, 1360 (1968)].
- ³⁰G. Szenes, *Nucl. Instrum. Methods Phys. Res. B* **146**, 420 (1998).
- ³¹J. M. Costantini, F. Brisard, A. Mcftah, F. Studer, and M. Toulemonde, *Radiat. Eff. Defects Solids* **126**, 233 (1993).
- ³²M. Toulemonde *et al.*, *Nucl. Instrum. Methods Phys. Res. B* **116**, 37 (1996).
- ³³T. A. Tombrello, *Nucl. Instrum. Methods Phys. Res. B* **83**, 508 (1993).
- ³⁴A. Meftah, M. Djebara, N. Khalfaoui, J. P. Stoquert, F. Studer, and M. Toulemonde, *Mater. Sci. Forum* **248-249**, 53 (1997).
- ³⁵We discuss here tracks which are amorphous. Results or conclusions on tracks with unidentified structure and origin are considered as nonrelevant to our subject.
- ³⁶G. Szenes, in *Atomistic Mechanisms in Beam Synthesis and Irradiation of Materials*, edited by J. C. Barbour, S. Roorda, D. Ila, and M. Tsujioka, *Mater. Res. Soc. Symp. Proc. No. 504* (Materials Research Society, Warrendale, PA, 1999), p. 111.
- ³⁷E. Seiberling, J. E. Griffith, and T. A. Tombrello, *Radiat. Eff.* **52**, 201 (1980).